Prenatal and lactational exposure to 2,3,7,8-tetrachlorodibenzo-p-dioxin (TCDD) impairs renal development in offspring of rhesus monkeys

Toshio Fukusato[1], Tatsumi Korenaga[1], Mari Ohta[2], Kazuo Asaoka[3], Hiroshi Sumida[4], Mineo Yasuda[4], Akihiro Arima[5], Suzuko Toida[6], Nobuo Murata[6], Shunichiro Kubota[2]

[1]Teikyo University School Of Medicine
[2]Graduate school of Arts and Sciences, The University of Tokyo
[3]Primate Research Institute, Kyoto University
[4]Faculty of Health Sciences, Hiroshima International University
[5]Shin Nippon Biomedical Laboratories, Ltd.
[6]Teikyo University School of Medicine, Mizonokuchi Hospital

Introduction

Exposure to 2,3,7,8-tetrachlorodibenzo-p-dioxin (TCDD) results in wide variety of effects including immunological dysfunction, teratogenicity and carcinogenesis1-4. In utero and lactational exposure to TCDD induces developmental abnormality in the brain and reproductive tissue of female offspring5, 6. Renal involvement by TCDD toxicity has been reported in rodents, horses, and cats7. Prenatal exposure to a high dose of TCDD is known to induce hydronephrosis in the mouse8. Considering the pronounced difference between species observed in some previous studies, effects of low dose of TCDD on development of the kidney in non-human primate were investigated in the present study after subcutaneous administration of TCDD into rhesus monkeys during pregnancy and lactation. The results showed a peculiar form of interstitial and peripelvic fibrosis with tubular and glomerular dysgenesis in the kidney of rhesus monkey offspring.

Materials and Methods

TCDD was purchased from Wellington Laboratories Inc., Guelph, Ontario, Canada) and was dissolved in a mixture of toluene/dimethylsulfoxide (DMSO;1:2, v/v) at Kanto Kagaku Co., Ltd. (Tokyo, Japan). Final concentrations were confirmed by gas chromatography. Colony bred adult female rhesus monkeys (age, 3-10 years; weight, 4-7kg) were purchased from China National Scientific Instruments & Materials Import/Export Corporation (Beijing, China).

TCDD (0, 30, 300ng/kg of body weight) was subcutaneously administrated to pregnant female monkeys on gestation day 20 (GD20), followed by injection with 5% of the initial dose every 30 days during pregnancy and lactation until GD90. Offspring that died by postnatal day (PND) 1100 were necropsied and examined macroscopically and histopathologically. Electron microscopic observation was also done. Renal tissue specimens were examined with quantitative image analysis (Win Roof, Mitani Corporation, Fukui, Japan) for fibrosis after picrosirius red stain. Immunohistochemical staining was performed on paraffin-embedded renal tissues using MAX-PO kitt (DakoCytomation, Glostrup, Denmark) and anti-vimentin (DakoCytomation), anti-alpha-smooth muscle actin (SMA) (DakoCytomation), anti-lymphocyte common antigen (LCA)(DakoCytomation) antibodies.

Results and Discussion

Numbers of dams in each group (0, 30, 300ng/kg) were 23, 20, and 20, respectively; live births, 18, 15, and 16; postnatal deaths, 6, 3, and 9. The cause of postnatal death included pneumonia in one monkey and renal failure in two. Renal interstitial and peripelvic fibrosis with or without atrophic papilla (Figure 1,2) was found in 5 (56%) of 9 offspring of dams exposed to relatively high dose of TCDD (300ng/kg), which were alive until PND1 to 465. The renal lesion was associated with renal tubular damage and function failure. Tubular and glomerular dysgenesis was also indicated. Electron microscopic observation showed interstitial collagen deposition and loss of renal tubuli. Quantitative image analysis disclosed significant increase in sirius-red positive areas within the renal cortex, medulla, and hilus. An immunohistochemical study revealed predominant proliferation of vimentin-positive fibroblasts, not SMA-positive myofiboblast, in these lesions. LCA-posive lymphocyte infiltration was minimal. No remarkable abnormalities were detected in the kidneys of 6 offsping of controls and 3 offspring of dams exposed to

relatively low dose (30ng/kg) of TCDD.

Although it has been reported that low doses of TCDD cause myocardial fibrosis in marmosets[9], severe renal fibrosis found in offspring of rhesus monkey in the present study might not be directly induced by TCDD transferred from dams into offspring via placental blood or breast milk[10]. But it might be rather a secondary change which might follow abnormal renal differentiation including dysgenesis or loss of nephrons because it is known that TCDD induces hydronephrosis without severe fibrosis in offspring of mice and, in addition, both renal dysgenesis and hydronephrosis without severe fibrosis is evident in kidneys of transgenic mouse models with developmental anomaly[11-13]. This study is ongoing. We will be able to examine renal changes in still alive offspring in the near future.

In conclusions, this is the first report that describes a peculiar form of renal interstitial and peripelvic fibrosis with nephron dysgenesis developed in offspring of rhesus monkeys exposed during prenatal and lactational period to TCDD. The renal lesions developed exclusively in offspring of dams exposed to relatively high dose (300ng/kg) of TCDD.

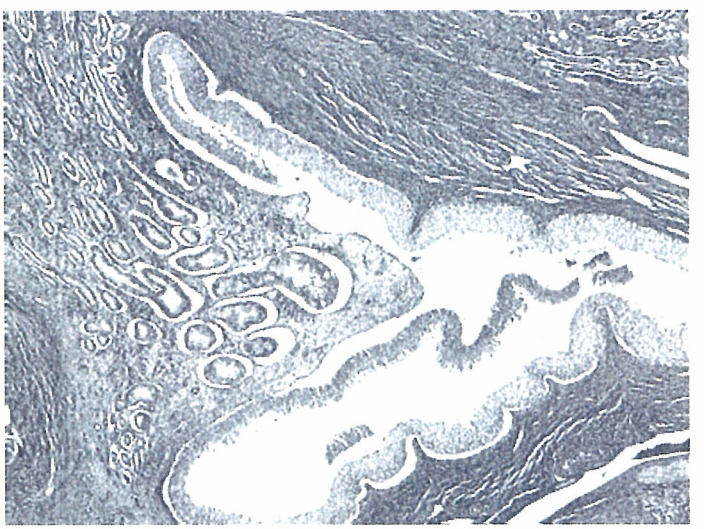

Figure 1. Interstitial and pericalyceal fibrosis with atrophic papilla in the kidney of rhesus monkey offspring.

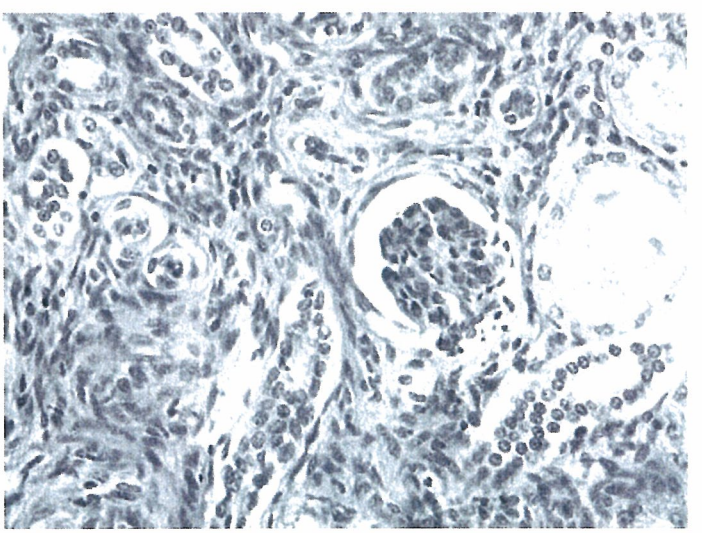

Figure 2. Interstitial fibrosis with sclerosing glomeruli and destruction or loss of renal tubuli in the kidney of rhesus monkey offspring.

Acknowledgement

This study is supported by Health Science Research Grants for Research on Environmental Health from the Ministry of Health, Welfare and Labor of Japan.

References

1. Colborn, T., vomSaal, F.S. and Soto, A.M. (1993) Environ. Health. Perspect. 101: 378-384.

2. Birnbaum, L.S. (1994) Environ. Health. Perspect. 102:157-167.

3. Sweeney, M.H. and Mocarelli, P. (2000) Food Addit. Contam. 17:303-316.

4. Signorini, S., Gerthoux, PM., Dassi, C., Cazzaniga, M., Brambilla, P., Vincoli, N. and Mocarelli, P. (2000) Andrologia 32:263-270.

5. Gray Jr. L. E., Wolf C., Mann P. and Ostby J. S. (1997) ToxicolApplPharm. 146:237-244.

6. MillerK. P., Borgeest C., Greenfeld C., Tomic D. and Flaws J. A. (2004) ToxicolApplPharm. 198:111-131.

7. Kimbrough R. D., Carter C. D., Liddle J. A. and Cline R. E. (1977) Arch Environ Health. 32:77-86.

8. Hassoun E., d'Argy R. and Dencker L. (1984) J Toxicol Environ Health. 14:337-351.

9. Riecke K., Grimm D., Shakibaei M., Kossmehl P., Schulze-Tanzil G., Paul M and Stahlmann R. (2002) Arch Toxicol. 76:360-366.

10. Shunichiro K., Ihara T., Oneda A., Inoue M., Sato M., Takasuga T., Yasuda M., Fukusato T., Hori H., Nomizu M. Kobayashi T. and Nagata R. (2001) Organohalogen Compounds 53:88-91.

11.Mendelsohn C., Batourina E., Fung S., Gilbert T. and Dodd J. (1999) Development 126:1139-1148.

12. Batourina E., Gim S., Bello N., Shy M., Clagett-Dame M., Srinivas S., Costantini F and Mendelsohn C. (2001) Nat Genet. 27:74-78.

13. Zhao H., Kegg H., Grady S., Truong H-T., Robinson M.L., Baum M. and Bates C.M. (2004) Dev Biol. 276:403-415.

Defects of the third molar teeth in rhesus monkeys prenatally and lactationally exposed to 2,3,7,8-tetrachlorodibenzo-p-dioxin (TCDD)

Mineo Yasuda[1], Iku Yasuda[1], Hiroshi Sumida[1], Akihiro Arima[2], Shunichiro Kubota[3]

[1]Department Of Clinical Radiology, Hiroshima International University
[2]Drug Safety Research Laboratories, Shin Nippon Biomedical Research Laboratories, Ltd.
[3]Department of Life Science, Graduate School of Arts and Sciences, The University of Tokyo

Introduction

Teeth are targets of developmental toxicity of dioxin. *In utero* and lactational TCDD exposure affects rat incisor and molar developmet[1,2]. In humans also tooth abnormalities were reported among populations exposed to dioxins[3]. We reported that pre- and postnatal exposure to TCDD affected development of deciduous and permanent teeth in rhesus monkeys[4]. The main abnormalities detected in stillborn and early postnatallyd died offspirng were missing deciduous incisors and molars. Observation upto approximatly 4 years of age revealed missing permanent incisors and premolars. In addition, cone-shaped or maldirected premolars were detected. This paper describes additional tooth findings in surviving 4.5-year-old offspirng .

Materials and Methods

Details of the materials and methods for this study are given elsewhere[4]. Briefly, adult female rhesus monkeys at the age of 5-7 years and weighing 4-6 kg were used. Female monkeys were mated with males for three days on days 12, 13, and 14 of the menstrual cycle. When copulation was confirmed visually, the median day of the mating periodwas disignated as day 0 of gestation (GD 0). On GD18 or 19, pregnancy was confirmed by an ultrasound device. Pregnant monkeys were divided into three groups, each consisting of approximately 20 animals. They were allowed to deliver naturally. The day on which delivery was detected was designated as postnatal day 0 (PND0). TCDD was dissolved in a mixture of toluene/DMSO (1:2, v/v) at a concentration of 300 ng/ml. Pregnant females were given TCDD subcutaneously into the back region on GD20 at an initial dose level of 30 or 300 ng/kg. The control animals received the vehicle in a volume of 1 ml/kg. For maintenance of a certain body burden, 5% of the initial dose, i.e. 0.6 or 6 ng/kg, was given to dams every 30 days during pregnancy andlactation until PND90.

Surviving offspring were examined at approximately 4.5 years of age for this study. They were anesthesized by intramuscular injection of ketamine at 10 mg/kg into the thigh before examination. Photographs were taken by an intraoral digital camera (Crystal Cam II, GC Co., Ltd., Tokyo). Conventional intraoral radiographs were taken by a portable X-ray apparatus (KX-60, Asahi Roentgen Ind. Co., Ltd., Kyoto) with a charge coupled device (CCD) (Gendex Visualix, Dentsply International Inc., York, PA, USA).

Results and Discussion

In addition to the abnormal dental findings reported previously[4], the present observation revealed missing third molars in the 300 ng/kg. In controls all the permanent teeth including the third molars were radiographically recognizable at 4.5 years of age, although the third molars were not fully erupted. Figure 1 is a radiograph of the right molar portion of the lower jaw of the offspring No. 1 (PND1718) in the control group. The first and second molars have been fully erupted, and their crowns with cusps and roots are clearly visible. Although only a mesial half of the third molar (arrow) appears in this radiograph, its already calcified crown is clearly observable. In contrast, at least two (No. 31, PND1710 and No. 66, PND1618) of the eight surviving offspring in the 300 ng/kg group had missing third molars. In the offspring No. 31, the third molars on the left side in the upper jaw and on both sides in the lower jaw were not seen in radiographs which include enough areas distal to the second molars. Figure 2 is a radiograph of the right molar portion of the lower jaw of the offspring No. 31. In the presumptive position of the third molar (arrow), neither calcified crown nor root is observable. The radiograph of the left upper jaw did not reveal the position of the third molar. In the offspring No. 66, the presence of the upper left third molar could be confirmed, whereas the lower right one was apparently missing. There were two other cases (No. 39, PND1690 and No. 44, PND1695) with

possible missing third molars which could not be definitely confirmed. The size of the CCD unit, 23 x 38 mm, is fairly large when compared with the size of the oral cavity of a rhesus monkey at the age of 4.5 years. Therefore it was not easy to get clear radiographs of the distal portion of the upper and lower dental arches by placing the unit on the labial side of the molars.

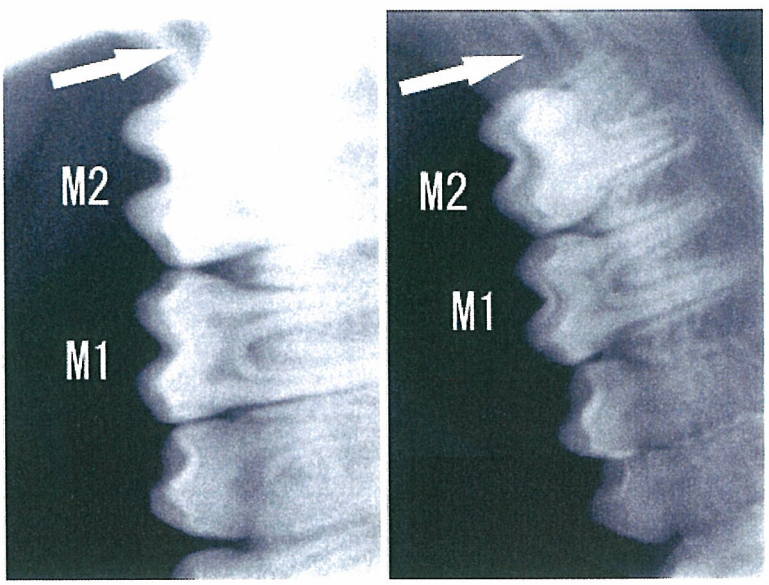

Figure 1.Lower right molars in No. 1 Figure 2. Lower right molars in No. 31

(Control group, PND 1718) (300 ng/kg group, PND 1710)

M1: the first molar; M2: the second molar; arrow: position of the third molar

The third molars in the rhesus monkey are still growing at the age of 4.5 years. Hence the final diagnosis of missing third molar should be done at the time of autopsy of these offspring.

In humans missing third molars are common among the general population. However, the third molars were invariably present in the parent monkeys used in the present study. Therefore missing third molars observed in the present study is considered to be caused by TCDD exposure.

Acknowledgements

This study was supported by Health Labour Science Research Grants for Research on Chemical Risk from the Ministry of Health Labour and Welfare of Japan.

References

1 Kattainen H., Tuukkanen J., Simanainen U., Tuomisto J.T., Kovero O., Lukinmaa P.-L., Alaluusua S., Tuomisto J.and Viluksela M. (2001) Toxicol. Appl. Pharmacol. 174, 216.

2 Kiukkonen A., Viluksela M., Shalberg C., Alaluusua S., Tuomisto J. T., Tuomisto J. and Lukinmaa P.-L. (2002) Toxicol. Sci. 69, 482.

3 Alaluusua S., Calderara P., Gerthoux P.M., Lukinmaa P.-L., Kover, O., Needham L., Patterson D. G., Jr., Tuomisto J. and Mocarelli P. (2004) Environ. Health Perspect. 112, 1313.

4 Yasuda I., Yasuda M., Sumida H., Tsusaki H., Arima A., Ihara T., Tsuga K. and Akagawa Y. (2005) Reprod.

Toxicol. 20, 21.

BENZENE-INDUCED HEMATOPOIETIC TOXICITY TRANSMITTED BY AHR IN THE WILD-TYPE MOUSE WAS NEGATED BY REPOPULATION OF AHR DEFICIENT BONE MARROW CELLS.

Yoko Hirabayashi[1], Byung-Il Yoon [1], Guang-Xun Li[1], Yoshiaki Fujii-Kuriyama[2], Toyozo Kaneko[1], Jun Kanno[1] and Tohru Inoue[3]

1 Division of Cellular and Molecular Toxicology and 3 Center for Biological Safety and Research National Institute of Health Sciences, Tokyo 158-8501, Japan.
2 Tsukuba Advanced Research Alliance (TARA) University of Tsukuba, Tsukuba 305-8577, Japan.

Introduction

Recent studies have shown that the aryl hydrocarbon receptor (AhR) in primitive cells transmits negative signals for the proliferation of such cells[1, 2]. As we previously reported, primitive hemopoietic progenitor cells increases in number in AhR-knockout (KO) mice; on the other hand, relatively mature progenitor cells on the other hand, decreases in number in a homeostatic manner[1].

We have reported that benzene-induced hemopoietic toxicity is transmitted by AhR[3]. We also found that cytochrome P450 2E1 (CYP2E1) related to benzene metabolism is also up regulated in the bone marrow by benzene exposure in the bone marrow[4]. Therefore, it is of interest to hypothesize a greater role of bone marrow cells in hemopoietic toxicities rather than the hepatic metabolism. Accordingly, in the present study, benzene-induced hemopoietic toxicity was evaluated in wild type (Wt) mice after a lethal dose of whole-body irradiation followed by repopulation of bone marrow cells that lack AhR or, *vice versa,* in AhR KO mice after repopulation of Wt bone marrow cells.

As results, benzene-induced hemopoietic toxicity seem to have been transmitted through AhR, and benzene was transformed by *de novo* metabolism with CYP2E1 in the bone marrow.

Materials and Methods

Animals. The establishment of homozygous AhR KO ($AhR^{-/-}$) mice, the 129/SvJ strain, is described elsewhere[3, 5]. The breeding of heterozygous AhR KO ($AhR^{+/-}$) males with $AhR^{+/-}$ females generated wild-type ($AhR^{+/+}$), $AhR^{+/-}$, and $AhR^{-/-}$mice. The neonates were genotyped by PCR screening of DNA from the tail. Female mice (12 weeks old) were used in the study. Eight-week-old C57BL/6 male mice from Japan SLC (Shizuoka, Japan) were used as recipients for the repopulation assay and the assay of CFU in the spleen. All the mice were housed under specific pathogen-free conditions at 24 ± 1°C and 55 ± 10%, using a 12-hr light-dark cycle. Autoclaved tap water and food pellets were provided *ad libitum.*

Blood and bone marrow (BM) parameters. Peripheral blood was collected from the orbital sinus. Peripheral blood leukocyte (WBC), red blood cell (RBC) and platelet (PLT) counts were determined using a blood cell counter (Sysmex M-2000, Sysmex Co., Kobe, Japan). Bone marrow (BM) cellularity was evaluated by harvesting BM cells from the femurs of each mouse[6]. The animals were sacrificed. Then a 27-gauge needle was inserted into the femoral bone cavity through the proximal and distal edges of the bone shafts, and BM cells were flushed out under pressure by injecting 2 ml of α-MEM. A single-cell suspension was obtained by gently triturating the BM cells through the 27-gauge needle, and cells were counted using Sysmex M-2000.

Irradiation. Recipient mice were exposed to a lethal radiation of 800.1 cGy, at a dose rate of 124 cGy/min, using a ^{137}Cs-gamma irradiator (Gamma Cell 40, CSR, Toronto, Canada) with a 0.5-mm aluminum-copper filter.

CFU-S Assay. The Till and McCulloch method[7] was used to determine the number of colony-forming units in the spleen (CFU-S). Aliquots of BM cell suspensions were used to evaluate the number of CFU-S. The number of BM cells was adjusted to that appropriate for producing nonconfluent spleen colonies, and the cells were then transplanted into lethally irradiated mice by injection through the tail vein. Spleens were harvested 9 and 13 days after the injection, and fixed in Bouin's solution. Macroscopic spleen colonies were counted under an inversion microscope at a magnification of ×5.6.

CFU-GM and CFU-E Assay. *in vitro* colony formation was assayed in semisolid methylcellulose culture[6,8]. Briefly, 8×10^4 BM cells suspended in 100 μl of medium were added to 3.9 ml of a culture medium containing 0.8% methyl cellulose, 30% fetal calf serum, 1% bovine serum albumin, 10^{-4} M 2-mercaptoethanol, with 10 ng/ml murine granulocyte-macrophage colony-stimulating factor (GM-CSF) for CFU-GM or 1 ng/ml murine Interleukin-3 and 2 U/ml erythropoietin for erythroid CFU (CFU-E). One-ml aliquots containing 2×10^4 BM cells were plated in triplicate in a 35-mm tissue-culture plate, and incubated for six days in a completely humidified incubator at 37 °C with 5% CO_2 in air. Colonies were counted under an inverted microscope at magnifications of ×40 for CFU-GM after 6-day culture and ×100 for CFU-E after 3-day culture.

BM repopulation assay[9]. The BM repopulation assay was performed similarly to the assay of CFU-S, except that 10^6 BM cells were injected into lethally irradiated mice. One month after the transfusion of BM cells, the repopulated mice were used in the experiment.

Results and Discussion

As previously reported, AhR-KO mouse showed a significant increase in WBC counts (**Figure 1** A). This was also consistent with the high number of myeloid progenitor cells, *i.e.*, CFU-S-9 and CFU-S-13, observed in the AhR-KO mice (**Figure 1** B). Thus, steady-state hemopoiesis is presumed to be suppressed by AhR signaling due to the possible presence of a physiological ligand, which is not readily observed in AhR-KO mice. In response to such an AhR-null effect, the AhR-KO mouse reversely shows extensive hemopoiesis in the spleen, although this hemopoietic enhancement is also reflected in another negative hemopoietic regulation in the BM. Accordingly, in the present study, benzene-induced hematotoxicity was evaluated in the Wt mice after a lethal dose of whole-body irradiation followed by the repopulation of BM cells that lack AhR.

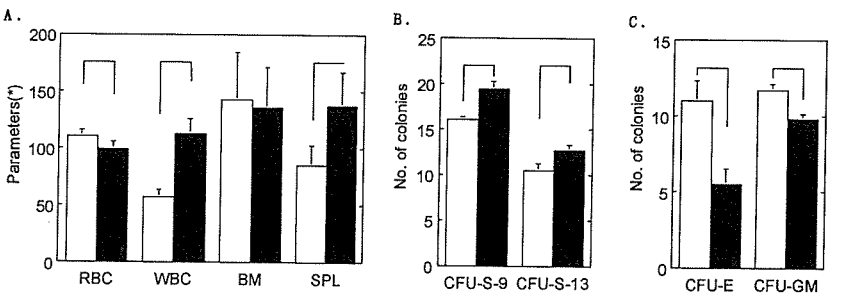

Figure 1: Comparison of various blood parameters between Wt mice (open columns) and AhR-KO mice (shaded columns) [1]; **A**. Peripheral blood, bone marrow and spleen weight. * Parameters indicate the counts of peripheral red blood cells (RBCs, $\times10^8$/ml) and white blood cells (WBCs, $\times10^6$/ml), bone marrow cellularity (BM, $\times10^5$/femur), and weight of spleen (SPL, mg). **B**. Number of colony-forming units in spleen (CFU-S/1$\times10^5$ BM cells) observed on days 9 (CFU-S-9) and 13 (CFU-S-13). **C**. Numbers of *in vitro* granulocyte-macrophage CFUs (CFU-GM/5$\times10^3$ BM cells) and erythroid CFU (CFU-E/1$\times10^4$ BM cells). †: Significant difference between Wt and AhR-KO mice determined by *t*-test at $p<0.05$.

Figures 2, A-C, show the RBC (A), WBC (B), and Plt (C) counts (per μL) in the peripheral blood after repopulation of the BM. In each figure, in the Wt mice repopulated with Wt BM cells (two columns on the left), the groups subjected to intraperitoneal benzene exposure (second from the left) show significant decreases in RBC and PLT counts (92% and 69%; p=0.010 and 0.016, respectively) compared with the sham exposure groups (farthest left in each figure), except 2B, i.e., WBC counts (96%). When the mice repopulated with AhR-KO BM cells (two columns on the right) are exposed to benzene, there are no significant differences between the sham exposure groups (second from the right) and the benzene exposed groups (farthest right) in A through C. Significant decreases observed in the Wt mice repopulated with Wt BM cells were negated when the Wt mice were repopulated with AhR-KO BM cells; thus, the reduction in the number of peripheral blood cells observed in the Wt mice after benzene exposure is assumed to be responsible for the AhR expression in BM cells. Although the two sham exposures (i.e., Wt mice, open column; and AhR-KO mice, solid column) are essentially identical in A and C, there seems to be insufficient recovery of the BM in transplantation in **Figure 2** B, and the solid column is significantly reduced (see, **Figure 3** on CFU-GM).

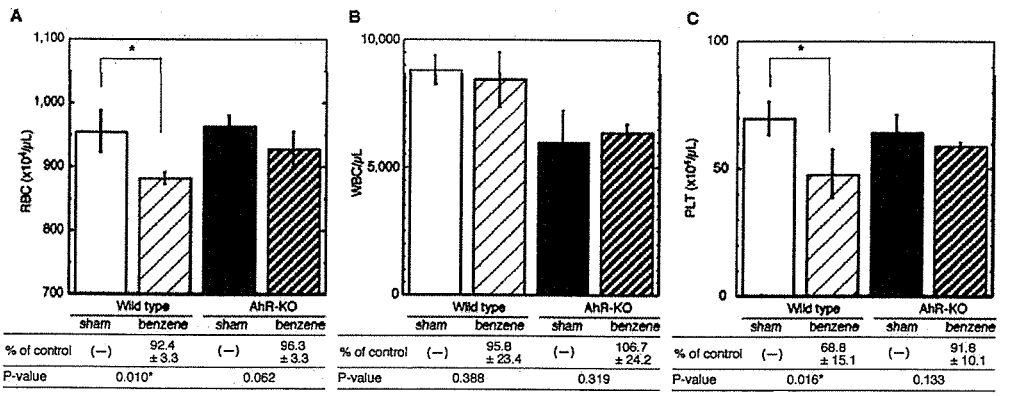

Figure 2: Comparison of various blood parameters in peripheral blood; A, RBC, B, WBC, and C, platelets (open bars vs lightly shaded bars in Wt mice repopulated with Wt BM cells; solid bars vs heavily shaded bars in Wt mice repopulated with AhR BM cells).

In Figure 3, again, the significant decrease in the number of granulocyte-macrophage colony-forming units *in vitro* (CFU-GM/5×10^3 BM cells) in the BM cells from the Wt mice repopulated with Wt BM cells (82.9% in benzene exposure, lightly shaded column to the right of the sham exposure, open leftmost column; p=0.041) is negated in the BM cells from mice repopulated with AhR-KO BM cells (sham exposure, solid column; and benzene exposure, heavily shaded column, respectively). In this figure, the efficiency of repopulation with AhR-KO BM cells (solid column) seems to be insufficient, since the solid column is smaller than the open column (p=0.025). The mechanism underling the incomplete recovery of AhR-KO BM cells, is still unknown; however, the sublethal irradiation of the recipient mice may be the case, where suppressive intrinsic factors may have been released from tissues given the lethal dose of irradiation received by the host animals.

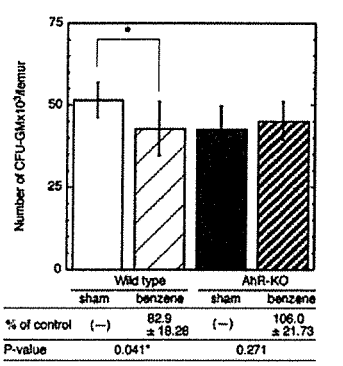

Figure 3: *:Significant difference between sham and exposed determined by *t*-test at p<0.05.

Despite the insufficient recovery of the number of GM-CFU in mice repopulated with

AhR-KO BM cells, number of BM cells, regardless of repopulated cell type (either Wt or AhR-KO BM cells) and type of exposure (either benene or sham exposure), there were no significant differences in number of BM cells among the groups in a homeostatic manner (**Figure 4** A; 91.4% and 92.4%, respectively, p>0.1). However, after benzene exposure, a significant decrease in splenic weight was observed in the Wt→Wt group (85.0%, p=0.022), but not in the AhR-KO-BM→Wt group (90.0%, p=0.173) (**Figure 4** B). This supports the notion that AhR-KO negates the suppressive effect on splenic weight after benzene exposure.

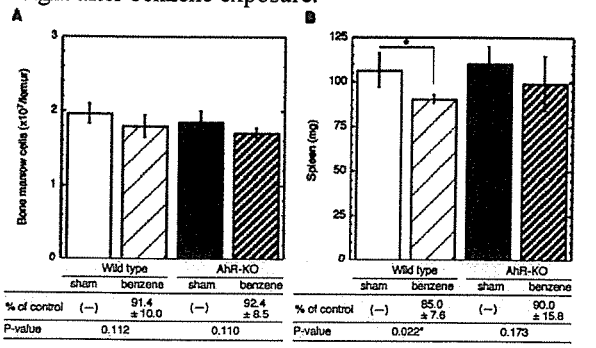

Figure 4: Comparison of number of BM cells (A) or weight of spleen (B) with or without benzene exposure, in mice repopulated with Wt BM cells or in mice repopulated with AhR-KO BM cells. (Wt mice repopulated with Wt BM cells, lightly shaded columns, second from left; or without benzene exposure, open columns, farthest left, benzene exposure vs Wt mice repopulated with AhR-KO BM cells, each of the two right columns).

Conclusions

The up-regulation of CYP2E1 after benzene exposure was specifically observed in our previous microarray study of the bone marrow tissue[4]. The analysis of the gene expression specifically derived from the hematopoietic stem cell compartment[10], and the evaluation of the toxicological alteration of such an expression as a measure of stem cell specific toxicological biomarkers are hot issues in the current hematotoxicology[11]. Mice that have been lethally irradiated and repopulated with BM cells from AhR-KO mice essentially did not shown any benzene-induced hematotoxicity, implying that such toxicity is derived from *de novo* metabolisms with CYP2E1 in the BM other than hepatic metabolism. The present study raises two questions on AhR-mediated TCDD-induced hematotoxicity: Do Wt mice repopulated with AhR-KO BM cells show hematotoxicity by TCDD unlike in the case of benzene exposure? If such is the case, what would be the transmitter from the site of xenobiotic metabolic activation to the bone marrow?

References

1 Hirabayashi, Y., Li, G., Yoon, B.I., Fujii-Kuriyama, Y., Kaneko, T., Kanno, J., and Inoue, T. (2003) Organohalogen Compounds, 64, 270
2 Garrett, R.W., and Gasiewicz, T.A. (2005) Meeting abstract [Molecular Regulation of Stem Cell, Keystone symosia], 61
3 Yoon, B.I., Hirabayashi, Y., Kawasaki, Y., Kodama, Y., Kaneko, T., Kanno, J., Kim, D.Y., Fujii-Kuriyama, Y., and Inoue, T. (2002) Toxicol Sci, 70, 150
4 Yoon, B.I., Li, G.X., Kitada, K., Kawasaki, Y., Igarashi, K., Kodama, Y., Inoue, T., Kobayashi, K., Kanno, J., Kim, D.Y., Inoue, T., and Hirabayashi, Y. (2003) Environ Health Perspect, 111, 1411
5 Mimura, J., Yamashita, K., Nakamura, K., Morita, M., Takagi, T.N., Nakao, K., Ema, M., Sogawa, K., Yasuda, M., Katsuki, M., and Fujii-Kuriyama, Y. (1997) Genes Cells, 2, 645
6 Yoon, B.I., Hirabayashi, Y., Kawasaki, Y., Kodama, Y., Kaneko, T., Kim, D.Y., and Inoue, T. (2001) Exp Hematol, 29, 278
7 Till, J.E., and McCulloch, E.A. (1961) Radiat Res, 14, 213
8 Hirabayashi, Y., Matsuda, M., Aizawa, S., Kodama, Y., Kanno, J., and Inoue, T. (2002) Exp Biol Med (Maywood), 227, 474
9 Hirabayashi, Y., Inoue, T., Suda, Y., Aizawa, S., Ikawa, Y., and Kanisawa, M. (1992) Exp Hematol, 20, 167
10 Ivanova, N.B., Dimos, J.T., Schaniel, C., Hackney, J.A., Moore, K.A., and Lemischka, I.R. (2002) Science, 298, 601
11 Hirabayashi, Y., Inoue, T. (2005) in: Handbook of Toxicogenomics (Borlak J., Ed.), Wiley-VCH Verlag GMbH & Co. Weinheim, 583.

J Toxicol Pathol 2005; 18: 41–46

Original

Electron Microscopical Evidence of the Protective Function of Thioredoxin (TRX/ADF) Transgene against 2,3,7,8-tetrachlorodibenzo-*p*-dioxin (TCDD)-induced Cellular Toxicity in the Liver and Brain

Byung-Il Yoon[1,5], Toyozo Kaneko[1], Yoko Hirabayashi[1], Takayoshi Imazawa[2], Akiyoshi Nishikawa[2], Yukio Kodama[1], Jun Kanno[1], Junji Yodoi[4], Jeong-Hee Han[5], Masao Hirose[2], and Tohru Inoue[3]

[1]Division of Cellular and Molecular Toxicology
[2]Department of Pathology
[3]Safety and Research Center of National Institute of Health Sciences, Tokyo 158–8501, Japan
[4]Department of Biological Responses, Institute for Virus Research, Kyoto University, Kyoto, Japan
[5]Department of Veterinary Medicine, Kangwon National University, Chunchcon 200–701, Korea

Abstract: The present study was performed to assess the protective role of thioredoxin/adult T-cell leukemia-derived factor (TRX/ADF) on the liver and brain cell damages induced by 2,3,7,8-tetrachlorodibenzo-*p*-dioxin (TCDD) in ADF wild-type (WT) and transgenic (Tg) mice. The ADF WT and Tg mice were intraperitoneally injected with a single dose of TCDD (150 μg/kg body weight). One day after the treatment, the liver and brain tissues were examined electron microscopically to evaluate the cellular toxicity. In the ADF WT mice, marked reduction of subcellular components, such as mitochondria, rough endoplasmic reticula, and glycogen granules, as well as swelling of the remaining mitochondria, were evident in the liver cells. However, attenuation of these changes was evident in TCDD-treated TRX/ADF mice. Similar subcellular changes noted in the neuronal cells of TCDD-treated WT mice were also attenuated in Tg mice. The results suggest that oxidative cellular damage contributes to the acute toxicity induced by TCDD and that TRX/ADF protects against it. (J Toxicol Pathol 2005; **18**: 41–46)

Key words: Ah receptor, brain, liver, 2,3,7,8-tetrachlrodibenzo-*p*-dioxin (TCDD), thioredoxin/adult T-cell leukemia-derived factor (TRX/ADF), transgenic (Tg) mouse

Introduction

As one of the aromatic hydrocarbons, 2,3,7,8-tetrachlorodibenzo-*p*-dioxin (TCDD) is a widely spread environmental pollutant that has a broad spectrum of toxic effects on a variety of tissues such as the thymus, liver, testes and central nervous system in mammals[1–6]. Although a number of studies have shown that the toxic effects of TCDD are mediated by intracytoplasmic aromatic hydrocarbon receptor (AhR)[7–9], the toxic mechanism of TCDD on the target organs is still not fully understood. Among the toxic events, oxidative stress is considered to play a major role in the toxic mechanism of TCDD, as characterized by marked increases of lipid peroxidation, the formation of reactive oxygen species, and DNA single-strand break[9–14].

Exogenous xenobiotics, such as aromatic hydrocarbons, result in profound induction of cytochrome P450 enzymes in the liver, resulting in the generation of reactive oxygen species[15,16]. On the other hand, the brain is rich in peroxidizable fatty acids and has relatively low catalase activity[17]. Therefore, these organs are considered to be highly susceptible to oxidative stresses[18]. In fact, the contribution of oxidative stress in TCDD-induced cellular damage of the liver and brain has been suggested in previous studies[13,18–22].

Adult T-cell leukemia-derived factor (ADF) is a human thioredoxin (TRX) associated with the reduction/oxidation (redox) regulation of the cellular environment[23]. TRX/ADF is a stress-inducible protein and its expression is up-regulated after viral infection as well as in cellular stress conditions induced by oxidative agents such as hydrogen peroxide or diamide, irradiation with X-rays and ultraviolet

Received: 24 September 2004, Accepted: 15 February 2005
Mailing address: Byung-Il Yoon, Department of Veterinary Medicine, College of Animal Resources Sciences, Kangwon National University, 192–1 Hyoja2-dong, Chunchcon, Kangwon 200–701, Republic of Korea
TEL: 82-33-250-8679 FAX: 82-33-244-2367
E-mail: byoon@kangwon.ac.kr

light, or ischemic reperfusion[23]. Previous studies have shown that TRX/ADF plays a role in the cellular defense mechanism against oxidative cellular damage via the regulation of intracellular redox status, since exogenously administered TRX/ADF protected cells from oxidative cellular injury[24,25].

We recently reported for the first time the protective function of TRX/ADF against TCDD-induced hematotoxicity in ADF transgenic (Tg) mice, indicating oxidative stress contributes to the hematotoxic mechanism of TCDD[26]. We hypothesized in the present study that overexpression of TRX/ADF might also be effective for protection against the toxic effects of TCDD on the liver and brain tissues in which oxidative stress has also been implicated in the toxic mechanism. For this purpose, we injected TCDD with a dosage capable of inducing oxidative stress in the liver following acute exposure[21], to ADF wild-type (WT) and transgenic (Tg) mice, and then compared subcellular changes electron microscopically in the liver and brain tissues.

Materials and Methods

Animals

TRX/ADF overexpressed mice (ADF Tg mice), originally produced by Dr. A. Mitsui[27], were maintained in a laboratory facility with a 12:12-hour light-dark cycle at an ambient temperature of 21 ± 2°C at the National Institute of Health Sciences (NIHS) of Japan by breeding ADF WT and Tg mice. Animals were screened by PCR of their tail DNA to determine their genotypes. At 8 weeks of age, male ADF WT and Tg mice (23.5–24.8 g) were transferred to a vinyl isolator established in a hazard room designed to prevent contamination from the outside environment and randomly allocated within the same genotype to housing with 6 animals per cage. A pelleted basal diet (CRF-1; Funabashi Farm, Funabashi, Japan) and tap water were provided *ad libitum* throughout the study.

Chemical

TCDD was obtained from Radian International, Cambridge Isotope Laboratories, Inc. (Andover, MA, USA; purity: 98 %). TCDD was initially dissolved in a small volume of acetone and subsequently adjusted to the concentration of 10 μg/ml in olive oil.

Experimental design

ADF WT and Tg mice were divided into vehicle controls and TCDD treatment groups, each consisting of 6 animals. After one week of acclimation, TCDD at 150 μg/kg was intraperitoneally injected once to animals of treatment groups, and the corresponding volume of olive oil was similarly injected to vehicle controls. The dosage of TCDD was selected based on previous study results that showed oxidative stress in the liver was induced by a single bolus injection to mice[21]. One day after the treatment, the animals were sacrificed by decapitation and then examined grossly. The liver and brain were then excised and their weights were measured.

The animal protocol was reviewed and approved by the Animal Care and Use Committee of the NIHS, Japan.

Morphological assessment

For histological examination, liver tissues in all animals were fixed in 10% neutral buffered formalin (pH 7.4). After routine processing, the paraffin-embedded sections were stained with hematoxylin and eosin and then examined histopathologically under a light microscope.

For electron microscopical examination, tissue specimens from the liver and cerebral cortex were respectively prepared from three animals each of the control and treatment groups of ADF WT and Tg mice. Small tissue blocks, sized 1 mm^3, were fixed with 2.5% glutaraldehyde in 0.2 M Sorenson's sodium phosphate buffer, pH 7.2, for 8 hours at 4°C. After washing with 0.1 M PBS (pH 7.4), the tissues were post-fixed with 1% osmium tetroxide for 90 minutes. After washing in 0.1 M PBS, the tissues were dehydrated with ethanol and propylene oxide and then embedded in Epon 812. Ultrathin sections were double-stained with uranyl acetate and lead citrate. The sections were examined with JEOL-1200 EX II electron microscope (JEOL, Tokyo, Japan).

Results

After one day of TCDD treatment, absolute liver weight had decreased to 71.4% of the vehicle control group in ADF WT mice and 83.2% in ADF Tg mice (data not shown).

Histologically, apoptotic liver cell debris and also focal liver cell necrosis were sparsely observed in the centrilobular areas of both TCDD-treated WT and ADF Tg mice, without showing apparent difference in the severity between genotypes (data not shown). Vehicle control animals did not show such liver cell changes in either genotype.

Electron microscopically, liver cells of the WT mice treated with TCDD exhibited a prominent decrease of cytoplasmic glycogen granules and rough endoplasmic reticula (RERs) and an increase of smooth endoplasmic reticula (SERs) (Fig. 1B). The number of mitochondria was also decreased and the remaining mitochondria showed swelling with disorganized cristae and lucent matrix. Increased fat droplets were also evident in the cytoplasm of less affected hepatocytes. On the other hand, transgene of Trx/ADF notably attenuated these morphological changes following TCDD treatment (Fig. 1C). In the cerebral cortex, neuronal cells showed a decrease in the number of RERs, ribosomes and mitochondria in WT mice treated with TCDD (Fig. 2B) but not in ADF Tg mice treated similarly with TCDD (Fig. 2C). Vehicle control animals did not show such neuronal cell changes in either genotype.

Discussion

In the present study, acute treatment with TCDD

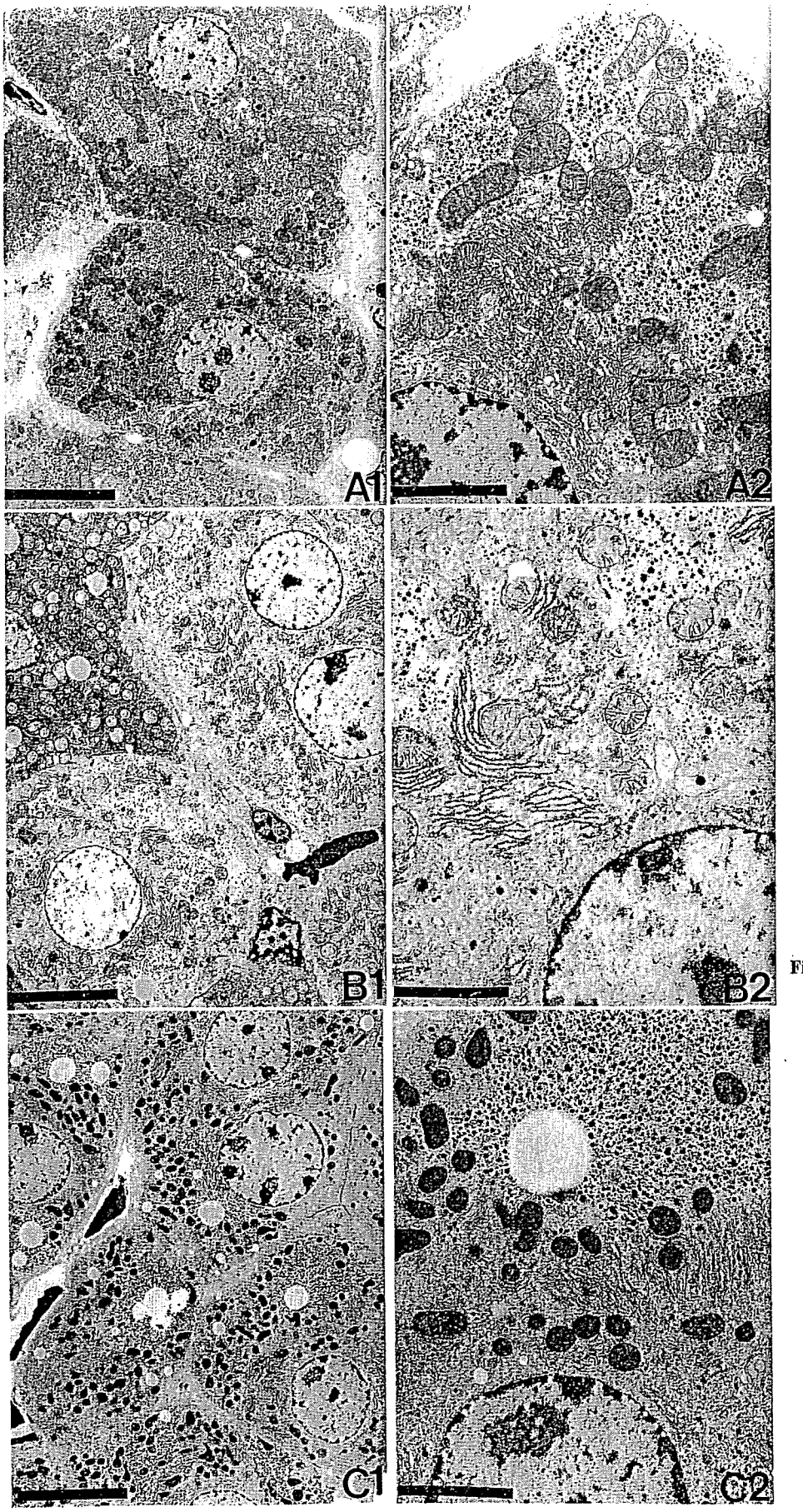

Fig. 1. Electron micrographs of liver cells from ADF WT and Tg mice treated with vehicle or TCDD. (A) Vehicle-treated ADF WT mouse, (B) TCDD-treated ADF WT mouse, and (C) TCDD-treated ADF Tg mouse. Note cytoplasmic swelling associated with a profound decrease of glycogen granules, RERs and mitochondria in the liver cells of the TCDD-treated ADF WT mouse (B). Swelling of the remaining mitochondria with disorganized cristae and lucent matrix is also evident (B). Attenuation of these morphological changes is evident in the TCDD-treated ADF Tg mouse (C). Uranyl acetate and lead citrate. Bar=10 μm (A1, B1, C1), Bar=3 μm (A2, B2, C2).

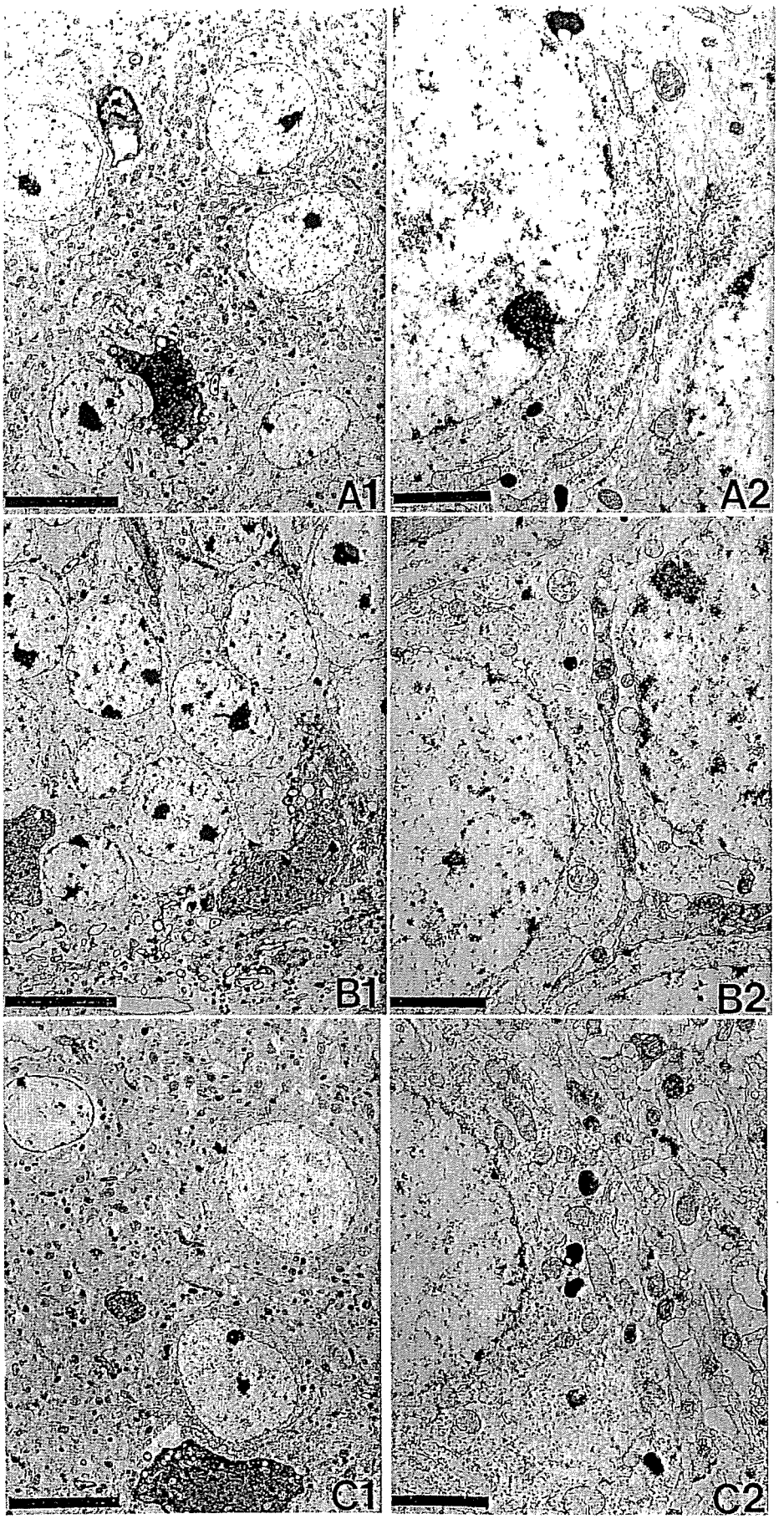

Fig. 2. Electron micrographs of neuronal cells in the cerebral cortex from ADF WT and Tg mice treated with vehicle or TCDD. (A) Vehicle-treated ADF WT mouse, (B) TCDD-treated ADF WT mouse, and (C) TCDD-treated ADF Tg mouse. Note the decrease of RER, ribosome and mitochondria in the cytoplasm of neuronal cells of the TCDD-treated ADF WT mouse (B). In the TCDD-treated ADF Tg mouse, mitochondrial swelling is also evident, but attenuation of the morphological changes can be seen, too. (C). Uranyl acetate and lead citrate. Bar=10 μm (A1, B1, C1), Bar=2 μm (A2, B2, C2).

induced ultrastructural alterations in the cytoplasmic components of liver cells characterized by prominent decrease of glycogen granules and RERs, proliferation of SERs, decrease and degradation of mitochondria, and increase of lipid droplets. These subcellular alterations were mostly consistent with those noted in the guinea pig liver following TCDD treatment[28], but concentric membrane arrays in the liver cells were not evident in the present study, presumably due to the different experimental protocol or the different species used in the studies. In the cerebral neuronal cells in the present study, alterations in subcellular components by TCDD were also evident, despite the changes being less profound than those in the liver cells. These subcellular changes in the liver and neuronal cells may represent the cytotoxic outcome of TCDD due to oxidative cellular damage and also cellular adaptation including detoxification.

Effective prevention of TCDD-induced toxicity by administration of antioxidants such as oltipraz[5-(2-pyrazinyl)-4-methyl-1,2-dithiol-3-thione] or butylated hydroxyanisole, or by pretreatment with vitamins A and E further supports the hypothesis that oxidative processes are involved in TCDD-induced toxicity[29,30]. Attenuation of subcellular changes in the liver and neuronal cells by transgene of TRX/ADF in the present study indicates the critical role of oxidative stress in the toxic events induced by TCDD, and also the protective function of ADF/TRX in these organs, as in our previous study of TCDD-induced bone marrow toxicity[26]. The protective effect of TRX/ADF against oxidative cellular damage is believed to be achieved by free radical scavengers[31], activation of DNA repair enzymes, such as activator protein endonuclease (Ref-1; redox factor-1)[32], and activation of nuclear factor-kappa B (NF-kB)[33].

Taken together, the results of our present study strongly suggest that the acute toxic effect induced in the liver and brain by a single large dose of TCDD is due to oxidative cellular damage, and that TRX/ADF plays a role in protection against TCDD-induced acute toxicity. Considering the routes and concentrations of TCDD exposed to humans, research on the effect of extremely low doses of TCDD by oral ingestion on the oxidative cellular damage of target organs is clearly warranted.

References

1. Kociba RJ, Keeler PA, Park CN, and Gehring PJ. 2,3,7,8-Tetrachlorodibenzo-*p*-dioxin (TCDD): results of a 13-week oral toxicity study in rats. Toxicol Appl Pharmacol. **35**: 553–574. 1976.
2. Chahoud I, Krowke R, Schimmel A, Merker HJ, and Neubert D. Reproductive toxicity and pharmacokinetics of 2,3,7,8-tetrachlorodibenzo-*p*-dioxin. 1. Effects of high doses on the fertility of male rats. Arch Toxicol. **63**: 432–439. 1989.
3. Funseth E and Ilbäck N-G. Effects of 2,3,7,8-tetrachlorodibenzo-*p*-dioxin on blood and spleen natural killer (NK) cell activity in the mouse. Toxicol Lett. **60**: 247–256. 1992.
4. Ivens IA, Loser E, Rinke M, Schmidt U, and Neupert M. Toxicity of 2,3,7,8-tetrachlorodibenzo-*p*-dioxin in rats after single oral administration. Toxicology. **73**: 53–69. 1992.
5. Ivens IA, Loser E, Rinke M, Schmidt U, and Mohr U. Sunchronic toxicity of 2,3,7,8-tetrachlorodibenzo-*p*-dioxin in rats. Toxicology. **83**: 181–201. 1993.
6. Erin Staples E, Murante FG, Fiore NC, Gasiewicz TA, and Silverstone AE. Thymic alteration induced by 2,3,7,8-tetrachlorodibenzo-*p*-dioxin are strictly dependent on aryl hydrocarbon receptor activation in hemopoietic cells. J Immunol. **160**: 3844–3854. 1998.
7. Poland A and Knutson JC. 2,3,7,8-Tetrachlorodibenzo-*p*-dioxin and related halogenated aromatic hydrocarbons: examination of the mechanism of toxicity. Annu Rev Pharmacol Toxicol. **22**: 517–554. 1982.
8. Cook JC, Gaido KW, and Greenlee WF. Ah receptor: relevance of mechanistic studies to human risk assessment. Environ Health Perspect. **76**: 71–77. 1987.
9. Alsarif NZ, Lawson T, and Stohs SJ. Oxidative stress induced by 2,3,7,8-tetrachlorodibenzo-*p*-dioxin is mediated by the aryl hydrocarbon (Ah) receptor complex. Toxicology. **92**: 39–51. 1994a.
10. Stohs SJ, Hassan MQ, and Murray WJ. Lipid peroxidation as a possible cause of TCDD toxicity. Biochem Biophys Res Commun. **111**: 854–859. 1983.
11. Mohammadpour H, Murray WJ, and Stohs SJ. 2,3,7,8-Tetrachlorodibenzo-*p*-dioxin -induced lipid peroxidation in genetically responsive and non-responsive mice. Arch Environ Contam Toxicol. **17**: 645–650. 1988.
12. Wahba ZZ, Lawson TA, Murray WJ, and Stohs SJ. Factors influencing the induction of DNA single strand breaks in rats by 2,3,7,8-tetrachlorodibenzo-*p*-dioxin (TCDD). Toxicology. **58**: 57–69. 1989.
13. Al-Bayati ZAF, Murray WJ, and Stohs SJ. 2,3,7,8-Tetrachlorodibenzo-*p*-dioxin-induced lipid peroxidation in hepatic and extrahepatic tissues of male and female rats. Arch Environ Contam Toxicol. **16**: 159–166. 1987.
14. Alsharif NZ, Schlueter WJ, and Stohs SJ. Stimulation of NADPH-dependent reactive oxygen species formation and DNA damage by 2,3,7,8-tetrachlorodibenzo-*p*-dioxin in rat peritoneal lavage cells. Arch Environ Contam Toxicol. **26**: 392–397. 1994b.
15. Stohs SJ. Oxidative stress induced by 2,3,7,8-tetrachlorodibenzo-*p*-dioxin (TCDD). Free Radic Biol Med. **9**: 79–90. 1990.
16. Bondy SC and Naderi S. Contribution of hepatic cytochrome P450 systems to the generation of reactive oxygen species. Biochem Pharmacol. **48**: 155–159. 1994.
17. Floyd RA. Antioxidants, oxidative stress, and degenerative neurological disorders. Proc Soc Exp Biol Med. **222**: 236–245. 1999.
18. Hassoun EA, Li F, Abushaban A, and Stohs SJ. Production of superoxide anion, lipid oxidation and DNA damage in the hepatic and brain tissues of rats after subchronic exposure to mixtures of TCDD and its congeners. J Appl Toxicol. **21**: 211–219. 2001.
19. Tritscher AM, Seacat AM, Yager JD, Groopman JD, Miller BD, Bell D, Sutter TR, and Lucier GW. Increased oxidative DNA damage in livers of 2,3,7,8-tetrachlorodibenzo-*p*-dioxin treated intact but not ovarectomized rats. Cancer Lett.

98: 219–225. 1996.

20. Hassoun EA, Wilt SC, Devito MJ, Van Birgelen A, Alsharif NZ, Birnbaum LS, and Stohs SJ. Induction of oxidative stress in brain tissues of mice after subchronic exposure to 2,3,7,8-tetrachlorodibenzo-*p*-dioxin. Toxicol Sci. **42**: 23–27. 1998.
21. Slezak BP, Hatch GE, DeVito MJ, Diliberto JJ, Slade R, Crisman K, Hassoun E, and Birnbaum LS. Oxidative stress in female B6C3F1 mice following acute and subchronic exposure to 2,3,7,8-tetrachlorodibenzo-*p*-dioxin (TCDD). Toxicol Sci. **54**: 390–398. 2000.
22. Senft AP, Dalton TP, Nebert DW, Genter MB, Hutchinson RJ, and Shertzer HG. Dioxin increases reactive oxygen production in mouse liver mitochondria. Toxicol Appl Pharmacol. **178**: 15–21. 2002.
23. Nakamura H, Nakamura K, and Yodoi J. Redox regulation of cellular activation. Annu Rev Immunol. **15**: 351–369. 1997.
24. Nakamura H, Matsuda M, Furuke K, Kitaoka Y, Iwata S, Toda K, Inamoto T, Yamaoka Y, Ozawa K, and Yodoi J. Adult T cell leukemia-derived factor/human thioredoxin protects endothelial F-2 cell injury caused by activated neutrophils or hydrogen peroxide. Immunol Lett. **42**: 75–80. 1994.
25. Yokomise H, Fukuse T, Hirata T, Ohkubo K, Go T, Muro K, Yagi K, Inui K, Hitomi S, and Mitsui A. Effect of recombinant human adult T cell leukemia-derived factor on rat lung reperfusion injury. Respiration. **61**: 99–104. 1994.
26. Yoon BI, Hirabayashi Y, Kaneko T, Kodama Y, Kanno J, Yodoi J, Kim DY, and Inoue T. Transgene expression of thioredoxin (Trx/ADF) protects against 2,3,7,8-tetrachlorodibenzo-*p*-dioxin (TCDD)-induced hematotoxicity. Arch Environ Contam Toxicol. **41**: 232–236. 2001.
27. Takagi Y, Mitsui A, Nishiyama A, Nozaki K, Sono H, Gon Y, Hashimoto N, and Yodoi J. Overexpression of thioredoxin in transgenic mice attenuates focal ischemic brain damage. Proc Natl Acad Sci USA. **96**: 4131–4136. 1999.
28. Turner JN and Collins DN. Liver morphology in guinea pigs administered either pyrolysis products of a polychlorinated biphenyl transformer fluid or 2,3,7,8-tetrachlorodibenzo-*p*-dioxin. Toxicol Appl Pharmacol. **67**: 417–429. 1983.
29. Hassan MQ, Stohs SJ, and Murray WJ. Inhibition of TCDD-induced lipid peroxidation, glutathione peroxidase activity and toxicity by BHA and glutathione. Bull Environ Contam Toxicol. **34**: 787–796. 1985.
30. Hassan MQ, Stohs SJ, and Murray WJ. Effects of vitamin E and A on TCDD-induced lipid peroxidation and other biochemical changes. Arch Environ Contam Toxicol. **14**: 437–442. 1985.
31. Tanaka T, Nishiyama Y, Okada K, Hirota K, Matsui M, Yodoi J, Hiai H, and Toyokuni S. Induction and nuclear translocation of thioredoxin by oxidative damage in the mouse kidney: independence of tubular necrosis and sulfhydryl depletion. Lab Invest. **77**: 145–155. 1997.
32. Walker LJ, Robson CN, Black E, Gillespie D, and Hickson ID. Identification of residues in the human DNA repair enzyme HAP1 (Ref-1) that are essential for redox regulation of Jun DNA binding. Mol Cell Biol. **13**: 5370–5376. 1993.
33. Schenk H, Klein M, Erdbrügger W, Dröge W, and Schulze-Osthoff K. Distinct effects of thioredoxin and antioxidants on the activation of transcription factor NF-kB and AP-1. Proc Natl Acad Sci USA. **91**: 1672–1676. 1994.

Effects of Aryl Hydrocarbon Receptor Signaling on the Modulation of Th1/Th2 Balance[1]

Takaaki Negishi,[2]* Yutaka Kato,* Osamu Ooneda,† Junsei Mimura,† Tomonari Takada,‡ Hidenori Mochizuki,* Masayuki Yamamoto,† Yoshiaki Fujii-Kuriyama,†‡ and Shoji Furusako[2]*

An orally active antiallergic agent, M50367, skews the Th1/Th2 balance toward Th1 dominance by suppressing naive Th cell differentiation into Th2 cells in vitro. Administration results in the suppression of IgE synthesis and peritoneal eosinophilia in vivo. In this report, we determined that M50354 (an active metabolite of M50367) was a ligand for the aryl hydrocarbon receptor (AhR); the immunological effects of this compound on in vitro Th1/Th2 differentiation from naive Th cells and Th1/Th2 balance in vivo were manifested through binding to AhR. These effects were completely abolished in AhR-deficient mice. AhR expression in the naive Th cell was significantly up-regulated by costimulation of TCR and CD28. Suppression of naive Th cell differentiation into Th2 cells via binding of M50354 to AhR was associated with inhibition of GATA-3 expression in Th cells. In addition, forced expression of a constitutively active form of AhR or activation of AhR by the addition of representative ligands suppressed naive Th cell differentiation into Th2 cells. Based on these results, we conclude that AhR functions as a modulator of the in vivo Th1/Th2 balance through activation in naive Th cells. *The Journal of Immunology,* **2005, 175: 7348–7356.**

The aryl hydrocarbon receptor (AhR)[3] is a ligand-activated transcription factor belonging to the basic-helix-loop-helix (bHLH)/period-AhR nuclear translocator-single-minded (PAS) transcription factor superfamily (1). AhR normally exists within the cytoplasm as part of a complex with multiple proteins, including heat shock protein (HSP) 90 (2), AhR-activated 9 (3), and p23 (4). Once a ligand enters the cell and binds AhR, the ligand-bound AhR complex translocates to the nucleus. AhR then forms a heterodimer with another bHLH-PAS protein, AhR nuclear translocator (Arnt), after dissociating from the HSP90-containing complex. Within the nucleus, the AhR/Arnt heterodimer binds to a specific sequence within the promoter of various target genes, designated a xenobiotic responsive element (XRE), to activate their expression (5).

Although the natural ligand of AhR is not known, polycyclic aromatic hydrocarbons, such as 2,3,7,8-tetrachlorodibenzo-*p*-dioxin (TCDD) and related compounds, can bind and activate the AhR. The interaction of these chemicals with AhR mediates a variety of toxic effects, including immune suppression, thymic atrophy, endocrine disruption, tumor promotion, and cell differentiation (6–10). The T cell-mediated immunological response is one of the most sensitive targets of TCDD toxicity (11).

We previously reported that oral administration of the synthetic compound M50367 (Fig. 1) inhibited the production of plasma IgE and pulmonary eosinophilia, resulting in the suppression of airway hyperresponsiveness in murine models of atopic asthma. In ex vivo experiments, while oral administration of M50367 reduced the production of IL-4 and IL-5 by Ag-restimulated splenocytes, it enhanced the production of IFN-γ (12). Treatment of naive Th cells with M50354, a hydrolyzed form of M50367 (Fig. 1), suppressed their in vitro differentiation into Th2 cells with a concomitant increase in the Th1 cell population (13). Thus, the antiallergic effects of this compound may be explained by a direct influence on the Th1/Th2 differentiation of naive Th cells. Although we have found M50367 induces expression of the cytochrome P450 1A1 enzyme (CYP1A1) in mouse liver (our unpublished data), the molecular mechanism underlying this immunomodulatory effect remains unclear.

In this study, we demonstrated that M50354 is an AhR agonist; the AhR signaling pathways activated by M50354 binding skews the Th1/Th2 balance toward Th1 dominance, resulting in immunological responses with antiallergic effects. Furthermore, we determined that the modulatory effects of M50354 on the Th1/Th2 balance were associated with reduced expression of GATA-3, a key factor for Th2 differentiation.

Materials and Methods

Chemicals

M50367 and M50354 (Fig. 1) were synthesized in our laboratory (12). M50354 was used for in vitro studies, and M50367 was used for in vivo studies because M50354 is an active metabolite of M50367 and has low bioavailability (12, 13). [^{3}H]M50354 was synthesized by Amersham Biosciences. 3-Methylcholanthrene (3MC), α-naphthoflavone (αNF), and β-naphthoflavone (βNF) were purchased from Wako Pure Chemical. Resveratrol was obtained from Calbiochem.

Antibodies

Anti-mouse-CD3 (145-2C11), FITC-conjugated anti-CD4 (GK1.5), PE-conjugated anti-IL-4 (11B11), and allophycocyanin-conjugated anti-IFN-γ (XMG1.2) Abs were obtained from BD Pharmingen. An anti-CD28 mAb

*Pharmaceutical Research Center, Mochida Pharmaceutical, Shizuoka, Japan; †Center for Tsukuba Advanced Research Alliance and Institute of Basic Medical Sciences, University of Tsukuba, Tsukuba City, Japan; and ‡Solution Oriented Research for Science and Technology, Japan Science and Technology Agency, Kawaguchi, Japan

Received for publication October 29, 2004. Accepted for publication September 21, 2005.

The costs of publication of this article were defrayed in part by the payment of page charges. This article must therefore be hereby marked *advertisement* in accordance with 18 U.S.C. Section 1734 solely to indicate this fact.

[1] T.T. and Y.F.-K. were supported in part by a grant from Solution Oriented Research and Technology, Japan Science and Technology Agency, Kawaguchi, Japan.

[2] Address correspondence and reprint requests to Dr. Shoji Furusako, Pharmaceutical Research Center, Mochida Pharmaceutical, Shizuoka 412-8524, Japan. E-mail address: furusako@mochida.co.jp

[3] Abbreviations used in this paper: AhR, Aryl-hydrocarbon receptor; bHLH, basic-helix-loop-helix; PAS, period-AhR nuclear translocator-single-minded; XRE, xenobiotic responsive element; Arnt, AhR nuclear translocator; TCDD, 2,3,7,8- tetrachlorodibenzo-*p*-dioxin; 3MC, 3-methylcholanthrene; αNF, α-naphthoflavone; βNF, β-naphthoflavone; CA, constitutively active; wt, wild type; m, murine; PSL, photostimulated luminescence; HPMC, hydroxyl-propyl-methylcellulose; PCB, polychlorinated biphenyl; CYP, cytochrome P-450.

0022-1767/05/$02.00

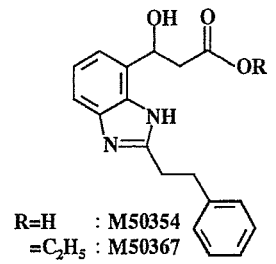

FIGURE 1. Chemical structures of M50354 and M50367.

(PV-1) was purchased from Southern Biotechnology Associates. Microbead-conjugated anti-FITC and anti-CD62L Abs were purchased from Miltenyi Biotec.

Construction of plasmids

A CYP1A1 luciferase reporter plasmid was constructed as follows. A full-length rat *CYP1A1* transcriptional regulatory region (−6300 to +2566) was prepared from pMC6.3k (14) by digestion with *Bgl*II and *Not*I and, after blunting, was end-cloned into the *Sma*I site of the pGL3-Basic vector (Promega) to give pMC6.3k-luc (see Fig. 2*A*).

A recombinant mouse AhR expression vector, wild-type (wt)-murine (m) AhR/pcDNA was constructed as follows. Mouse *AhR* cDNA fragment was amplified from C57BL/6 mouse liver cDNA by using the primers 5′-GGGTCTAGA^{-15}AGGGCGCGGGGCACCATGAG^{+5}-3 and 5′-GGG CTCGAG^{+2463}GAAAACACCTCAACTCTGCACCTTG^{+2427}-3′. The resultant PCR fragment was digested with *Xba*I and *Xho*I, and ligated to the *Xba*I and *Xho*I site of pcDNA3.1$^+$ (Invitrogen Life Technologies).

A constitutively active AhR (CA-AhR) was constructed as described by McGuire et al. (Ref. 15; see Fig. 6*A*). Two cDNA fragments of *AhR*, corresponding to aa 1–276 and 419–805, were amplified by PCR. Primers were designed to carry restriction sites for *Xba*I and *Bam*HI (1–276), and *Bam*HI and *Xho*I (419–805). The resulting fragments were digested with *Xba*I and *Bam*HI (1–276) or *Bam*HI and *Xho*I (419–805), and subcloned into *Xba*I-*Xho*I sites of pBluescript II KS$^+$ to give CA-mAhR/pBS.

pMSCV retroviral vector was a kind gift of Dr. A. Kume (Jichi Medical School, Tochigi, Japan). CA-mAhR/pBS or wt-mAhR/pcDNA was digested with *Xba*I and *Xho*I, and then blunt-ended with T4 DNA polymerase. The resulting fragments were ligated to the blunted *Xba*I site of pMSCV to generate wt-mAhR-RV or CA-mAhR-RV.

pBSK-mAhR was constructed by inserting the 2.5-kb *Xho*I-*Xba*I fragment of mAhR cDNA described in Ema et al. (16) into the *Xho*I/*Xba*I sites of pBluescript II SK$^+$.

Luciferase reporter assay

Before transfection, Hepa-1c1c7 cells were seeded in 96-well plates at 0.6×10^4 cells/well, then incubated at 37°C for 24 h. The cells were then transfected with the pMC6.3k-luc plasmid (30 ng/well) using FuGENE 6 transfection reagent (Roche Diagnostics). After 24 h of transfection, cells were treated for 24 h with a variety of compounds at indicated concentrations. Luciferase activity was then measured by using a PicaGene assay system (Wako Pure Chemical Industries).

EMSA

A double-stranded oligonucleotide XRE probe (17) was end-labeled with [γ-^{32}P]ATP (Amersham Bioscience) by T4 polynucleotide kinase (NEB) and purified by using ProbeQuant G-50 microcolumns (Amersham Biosciences). In vitro-translated mouse AhR and Arnt were prepared by the TnT T7 quick-coupled transcription/translation system (Promega), according to the manufacturer's instruction, using pBSK-mAhR and pBSK-mArnt (18), respectively.

An unprogrammed transcription/translation system (9 μl) or in vitro-translated mouse AhR and Arnt (4.5 μl) were mixed with vehicle (1 μl of DMSO) or chemicals and incubated for 2 h at 30°C. The reaction mixtures were combined with 10 μl of 2× binding buffer (200 mM HEPES-KOH (pH 7.9), 1 M KCl, 2 mM EDTA, 60 mM $MgCl_2$, 6% glycerol, 20 mM DTT, 0.2 mg/ml sonicated salmon sperm DNA, and one of the chemicals). After incubation for 20 min at 25°C, the radiolabeled XRE probe (2×10^4 cpm) was added and incubated for 20 min at 25°C. The reaction mixtures were applied onto 4.8% acrylamide gel in 0.5× Tris-borate-EDTA buffer. After the electrophoresis, the gel was processed on a gel dryer and then protein-DNA interaction was visualized and quantified with the BAS-1500 bio-image analyzing system (Fujifilm). The intensities of the bands were expressed as units of photostimulated luminescence (PSL).

Binding assay

Hepatic cytosols were prepared essentially as described previously (19). Mouse hepatoma cells, Hepa 1c1c7, were grown in modified αMEM supplemented with 10% FBS, sodium bicarbonate, and penicillin/streptomycin. The cells were harvested homogenized in HEDG buffer (25 mM HEPES, 1.5 mM EDTA, 1 mM DTT, 10% glycerol, pH 7.6 adjusted). For preparation of cytosols, membranes were removed by a 45 min centrifugation at 100,000 × g, and then the supernatant was stored at −70°C until use.

Specific binding of M50354 to AhR was assessed by trapping of the AhR complex using anti-AhR Ab. Briefly, 1 μl of ^{3}H-labeled M50354 (60 μM in ethanol) and a competitor (60 mM in DMSO) were added to 100-μl aliquots of cytosols (2.0 mg/ml), and then incubated for overnight at 4°C. These mixtures were added to 96-well microplates coated with the anti-AhR Ab (10 μg/ml), and incubated for 2 h at 4°C. These microplates were washed three times with HEDG buffer, and the retained radioactivities were measured using a scintillation counter.

Mice

C57BL/6 mice were obtained from Japan SLC. AhR-deficient ($AhR^{-/-}$) mice (20) were backcrossed with the C57BL/6 strain by 10 generations. The deficient mice were maintained as heterozygous mice in our laboratory. Mating $AhR^{+/-}$ males with $AhR^{+/-}$ females generated $AhR^{+/+}$, $AhR^{+/-}$ and $AhR^{-/-}$ mice. In the following experiments, we used the wt ($AhR^{+/+}$) and homozygous mutant mice ($AhR^{-/-}$) of the littermates. The neonates were genotyped by PCR of DNA from the tail. The sense primer for the wt at the 5′ region of the *AhR* gene was 5′-CGCGGGCACCAT GAGCAG-3′. The antisense primer for intron 1 was 5′-GAGACT CAGCTCCTGGATGG-3′. The same 5′ primer was used as for the mutant type, while the antisense primer for the *LacZ* gene was 5′-CGCCGAGT TAACGCCATCAA-3′. All in vivo animal experiments were approved by the Institutional Animal Use Committee of our institute.

Evaluation of Th1/Th2 balance in vivo

Mice were given 10 μg of DNP-*Ascaris* adsorbed with 4 mg of alum i.p. on day 0. The sensitized mice were orally treated from days 0 to 9 with 100 mg/kg M50367 or vehicle alone (0.5% hydroxyl-propyl-methylcellurose (HPMC): 10 ml/kg). On day 10, plasma samples were obtained to measure total plasma IgE levels by the sandwich ELISA method described by Hirano et al. (21). Subsequently, spleens were collected, and homogenized using a glass homogenizer under sterile conditions. Homogenates were centrifuged at 300 × g for 7 min at 4°C and cell pellets were resuspended in RPMI 1640 medium. The cell suspensions were filtered through 40 μm pore size nylon sieves to remove large cell aggregates. The isolated splenocytes were washed twice in the modified RPMI 1640 medium (S-Clone SF-B; Sanko Junyaku) and resuspended in S-Clone SF-B. One milliliter containing 5×10^6 cells was seeded onto 48-well plates and cultured in the presence of 10 μg/ml DNP-*Ascaris* for 18 h at 37°C. The culture supernatants were harvested and stored at −80°C until cytokine determination. IL-4, IL-5, and IFN-γ concentrations in the supernatants were measured using a commercial ELISA kit.

Ag-induced cell infiltration to the peritoneal cavity

Mice were given 10 μg of DNP-*Ascaris* i.p. on day 0. This injection was repeated on day 7, and the sensitized mice were orally given 100 mg/kg/day M50367 or vehicle alone (0.5% HPMC, 10 ml/kg/day) from days 0 to9. On day 10, the peritoneal cells were harvested by lavage (3 ml of saline containing 1% EDTA), and the total cell number was counted with a hemocytometer (Sysmex).

Naive Th cell preparation and evaluation of Th1/Th2 balance in vitro

Naive CD4$^+$CD62L$^+$ Th cells were prepared from murine spleens as described (22, 23). Briefly, splenocytes were treated with FITC-conjugated anti-CD4 mAb (GK1.5) and microbead-conjugated anti-FITC Ab, and then the microbead-labeled CD4$^+$ Th cells were separated by MACS. After washing, the microbeads were cleaved enzymatically. CD4$^+$CD62L$^+$ Th cells were then isolated using microbead-conjugated anti-CD62L mAb (MEL-14) using the MACS system. The obtained cells were confirmed to be >95% pure CD4$^+$CD62L$^+$ Th cells by flow cytometry.

The naive Th cells were seeded at 0.25×10^6 cells/ml in the plates containing immobilized anti-CD3 mAb (5 μg/ml). These cells were cultured in RPMI 1640 medium containing 10 mM HEPES (pH 7.4), 10%

FBS, 100 U/ml penicillin, 0.1 mg/ml streptomycin, 50 μM 2-ME, and 1 μg/ml anti-CD28 mAb. Three days after the stimulation, a portion of the culture supernatant was sampled for ELISA, and then the cells were expanded 3-fold in a fresh medium. On day 6, Th cells were stimulated again with immobilized anti-CD3 mAb for 6 h in the presence of 4 μM monensin to prevent the release of cytokines. After being stained with FITC-conjugated anti-CD4 mAb (GK1.5/4), the restimulated Th cells were sequentially permeabilized and fixed with Cytofix/CytoPerm (BD Pharmingen). Intracellular cytokines were detected with allophycocyanin-conjugated anti-IFN-γ (XMG1.2) and PE-conjugated anti-IL-4 (11B11) Abs, as described by the manufacturer's protocol (BD Pharmingen). Flow cytometric analysis was performed using FACSCalibur and CellQuest software (BD Biosciences). The axes were set such that the total positive population of isotype control may be below 1%.

Retroviral transduction

A retroviral packaging cell line, phenix (eco) cell, was transfected with CA-mAhR-RV or wt-mAhR-RV using FuGENE6. After 4 or 5 days of culture, PT67 cells (24) were infected with the supernatants from transfected phenix cells. Bright GFP-positive PT67 cells were selected for the preparation of high titer retroviral production cells.

Naive $CD4^+CD62L^+$ Th cells were activated as described above and infected on days 2 and 4 with solutions containing viral supernatant and 6 μg/ml polybrene (Sigma-Aldrich) at a 1:1 volume ratio. The cells were grown for 5 days after the primary activation, and intracellular cytokine staining was performed as described above.

Western blot analysis of AhR

Naive $CD4^+$ Th cells were activated as described above. At 24, 48, and 72 h after activation, the cells were harvested, washed with PBS^-, and lysed in SDS sample buffer (Daiichi Pure Chemicals) for 10 min at 99°C. The protein concentrations were measured by DC Protein Assay (Bio-Rad). Total proteins (10 μg) were separated by 7.5% SDS-PAGE, and then transferred to Fluorotrans W membrane filters (Pall Gelman Laboratory). The membrane filters were incubated with a rabbit polyclonal anti-AhR Ab (BIOMOL) or a rabbit polyclonal anti-Zap70 Ab (Santa Cruz Biotechnology), followed by detection with secondary peroxidase-conjugated anti-rabbit immunoglobulins (DakoCytomation). Signals on the filters were visualized with ECL plus Western blot detection reagent (Amersham Bioscience).

Quantitative transcript analysis

Total RNA was prepared from cultured cells using TRIzol reagent. Quantitative real-time PCR assay was performed using gene-specific primers and SYBR Green RT-PCR Reagent or TaqMan One-step RT-PCR Master Mix Reagent (Applied Biosystems) on a 7000 Sequence Detector (Applied Biosystems). The following pairs of primers and TaqMan probe were used for the RT-PCR assay: *GATA-3* in TaqMan RT-PCR, forward 5′-CA GAACCGGCCCCTTATCA-3′, reverse 5′-CAGGATGTCCCTGCTCTC CTT-3′, and TaqMan probe, 5′-6FAM-TGGCCCCAGCATGCGACCTC-TAMRA-3′; *T-bet*, in SYBR Green RT-PCR, forward 5′-TGCCAGG GAACCGCTTATAT-3′ and reverse 5′-GTTGGAAGCCCCCTTGTTGT-3′. c-*maf*, in SYBR Green RT-PCR, forward 5′-AAGGAGGAG GTGATCCGACT-3′ and reverse 5′-TCTCCTGCTTGAGGTGGTCT-3′. Results were normalized to expression of *β-actin*: forward 5′-GCTCTG GCTCCTAGCACCAT-3′, reverse 5′-GTGGACAGTGAGGCCAGGAT-3′, and TaqMan Probe, 5′-6FAM-TCAAGATCATTGCTCCTCCT GAGCGC-TAMRA-3′. The means ± SD of triplicate determinations are shown.

Statistical analysis

Results were evaluated by Dunnett's procedure for multiple comparisons or Student's *t* test using STAT LIGHT 1997 (Yukms). A difference among groups was considered to be significant when $p < 0.05$.

Results

Binding of M50354 to AhR and enhancement of CYP1A1 promoter activity

As oral administration of M50354 or M50367 induced CYP1A1 expression in mouse liver, we hypothesized that M50354 was an AhR ligand. To confirm this assumption, we examined the in vitro effect of M50354 on CYP1A1 induction, a common property of AhR agonists, in mouse hepatocytes. Hepa1c1c7 cells transiently transfected with pMC6.3k-luc were treated with a variety of concentrations of either M50354 or control compounds for 24 h. We then determined the expression levels of the inducible reporter gene. We observed that M50354 was a relatively weak inducer of CYP1A1, with an EC_{50} greater than 3×10^{-4} M (Fig. 2*A*). Due to a low solubility, we could not test the induction activities of M50354 at concentrations >300 μM. The EC_{50} values for the reference compounds βNF and αNF were estimated to be $\sim 3 \times 10^{-7}$ M and $\sim 1 \times 10^{-5}$ M, which were 3 and 2 orders of magnitude less than that of M50354, respectively. In contrast, resveratrol (25), a control AhR antagonist, had no effect on *CYP1A1* promoter activity at any of the concentrations tested.

To examine whether the addition of M50354 transformed AhR into an active form allowing the interaction with the XRE enhancer sequence, we performed EMSA. In vitro-translated mouse AhR and Arnt were mixed with the radiolabeled XRE probe and several concentrations of M50354. Addition of M50354 induced the formation of an AhR/Arnt/XRE complex in a dose-dependent manner at concentrations exceeding 10 μM (359 PSL at 10 μM, 1204 PSL at 30 μM, and 3601 PSL at 100 μM) (Fig. 2*B*). This result correlates with the induction activity of M50354 in luciferase assays. The reference compounds, 3MC and βNF, also promoted the interaction of AhR/Arnt complex with the XRE at 1 μM (3005 PSL at 1 μM 3MC, 1985 PSL at 0.3 μM βNF, and 2570 PSL at 1 μM βNF); these shifted bands disappeared with competition from excess unlabeled XRE probe. The ability of M50354 to form an AhR/Arnt/XRE complex was relatively weak, which is consistent with its ability to induce *CYP1A1* expression.

To investigate whether M50354 binds AhR, Hepa-1c1c7 cytosol was mixed with 0.6 μM [^{3}H]M50354, then incubated in 96-well plates with an immobilized anti-AhR Ab. After washing, the retained radioactivity was measured. Higher levels of radioactivity were detected in plates with immobilized anti-AhR Ab; this radioactivity could be abolished by the addition of excess competitor, such as unlabeled M50354, αNF, βNF, or 3MC (Fig. 2*C*). This result clearly demonstrated that M50354 specifically binds the AhR protein in a manner similar to other representative AhR ligands.

These results indicate that AhR was activated by M50354 binding. An enhancement of *CYP1A1* promoter activity followed this activation, although this enhancement was not as potent as that induced by αNF, a known partial agonist.

Requirement of AhR for the antiallergic effects of M50367 in vivo

To examine the requirement of AhR in the antiallergic effects mediated by M50367, we administered M50367 to $AhR^{-/-}$ mice.

We first investigated the effects of M50367 on plasma IgE levels in Ag-sensitized mice. $AhR^{-/-}$ and wt mice were sensitized by an i.p. injection of 10 μg of DNP-*Ascaris*/Almu on day 0. Sensitized mice were then treated orally with M50367 (100 mg/kg, daily) for 10 days, beginning on day 0. Orally administered M50367 inhibited IgE production with an EC_{50} value of 1–3 mg/kg (12). Despite the efficacy of low concentrations in this model, however, we used a dosage of 100 mg/kg/day to make the effects of M50367 in $AhR^{-/-}$ mice clear.

Irrespective of AhR genotype, plasma IgE levels in sensitized mice were elevated to levels ~2-fold higher than those observed in nonsensitized mice (Fig. 3*A*). Although the administration of M50367 to wt mice lowered the plasma IgE levels significantly (from 423 ng/ml to 67 ng/ml, $p < 0.01$), this suppression was not observed in $AhR^{-/-}$ mice. The Ag-sensitized $AhR^{-/-}$ mice exhibited 2.5-fold higher serum IgE levels than the wt animals (Fig. 3*A*), although the underlying mechanism remains unclear.

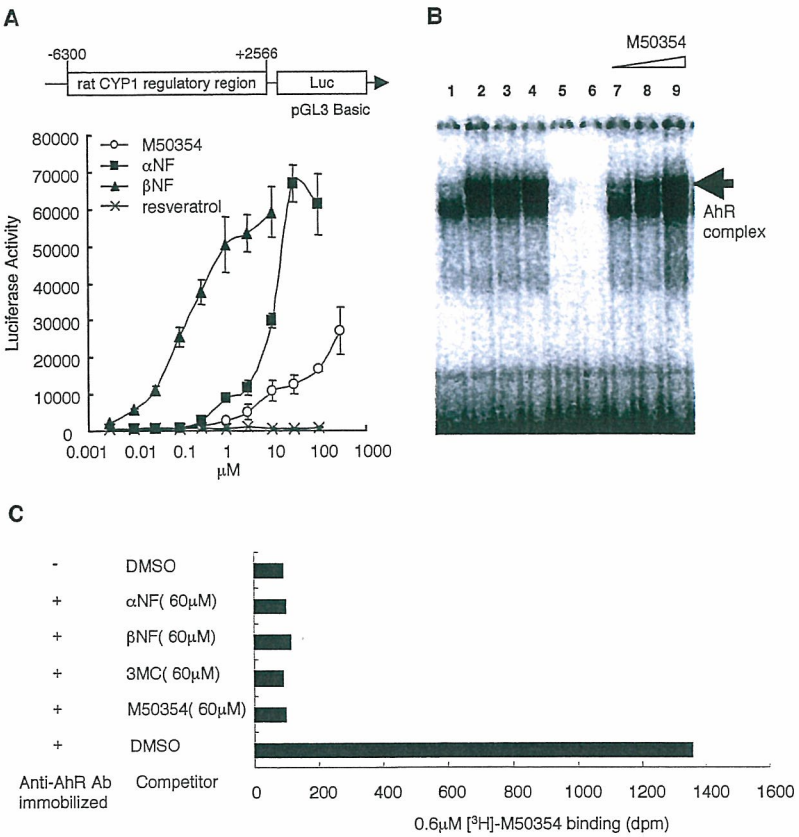

FIGURE 2. M50354 binds to AhR to enhance CYP1A1 promoter activity. *A*, Before transfection, Hepa-1c1c7 cells were seeded in 96-well plates at 0.6×10^4 cells/well, then incubated at 37°C for 24 h. The cells were then transfected with the pMC6.3k-luc plasmid (30 ng/well), the rat CYP1A1 promoter region (−6300 to +2566) ligated with the pGL3 Basic vector, using FuGENE 6 transfection reagent. Twenty-four hours after transfection, cells were treated for 24 h with a variety of compounds at the indicated concentrations. Luciferase activity was then measured using a PicaGene assay system. The means ± SD of quadruplicate determinations are shown. M50354 (○), βNF (▲), αNF (■), resveratrol (x). Data are representative of four independent experiments. *B*, In vitro-translated mouse AhR and Arnt were mixed with either vehicle (1 μl of DMSO) or the indicated chemicals, then incubated for 2 h at 30°C. We then performed EMSA with radiolabeled XRE probe (2×10^4 cpm). *Lanes*: *1*, DMSO control; *2*, 1 μM 3MC treatment; *3*, 0.3 μM βNF treatment; *4*, 1 μM βNF treatment; *5–6*, 1 μM βNF in the presence of a 30- or 100-fold excess of unlabeled XRE probe, respectively; *7–9*, 10, 30, and 100 μM M50354 treatment, respectively. *C*, Cytosols prepared from Hepa-1c1c7 cells were incubated with 0.6 mM [^{3}H]M50354 (37kBq) and competitor (100-fold excess) overnight at 4°C. Samples were added to anti-AhR Ab-coated 96-well plates and incubated for 2 h at 4°C. After washing with PBS$^-$, the retained radioactivity was measured by scintillation.

We then investigated the effects of M50367 on the increases in peritoneal cells induced by repeated Ag sensitization. AhR$^{-/-}$ and wt mice were sensitized twice by i.p. injection of 10 μg of *Ascaris* extract on days 0 and 7. Mice were given M50367 orally (100 mg/kg, daily) for 10 days beginning on day 0, after which the number of peritoneal exudate cells was counted. Although administration of M50367 significantly suppressed the total number of peritoneal exudate cells in the wt mice (from 13.8×10^6 cells to 7.9×10^6 cells, $p < 0.05$), no suppression was observed in *AhR*$^{-/-}$ mice. Ag-sensitized *AhR*$^{-/-}$ mice exhibited a small, but significant, increase in the number of peritoneal exudate cells from the levels observed in their wt counterparts (Fig. 3*B*). This increase in cell number may be related to the elevated serum IgE levels in *AhR*$^{-/-}$ mice.

To evaluate the effects of M50367 on Th1/Th2 balance, we measured cytokine production by ex vivo restimulated splenocytes. In wt splenocytes, the enhanced levels of IL-5 induced by DNP-*Ascaris* sensitization were reduced by treatment with M50367 (from 332 pg/ml to 107 pg/ml, $p < 0.01$), while IFN-γ production was enhanced by M50367 treatment (from 334 pg/ml to 3310 pg/ml, $p < 0.01$) (Fig. 3, *C* and *D*). This result indicated that M50367 administration skewed the Th1/Th2 balance toward Th1 dominance in wt mice. In contrast, M50367 had no effect on either IL-5 or IFN-γ production in *AhR*$^{-/-}$ mice. Interestingly, sensitized *AhR*$^{-/-}$ mice exhibited 3-fold higher IL-5 levels than wt animals treated in a similar manner (Fig. 3, *C* and *D*). Even higher increases in IFN-γ production were observed in sensitized *AhR*$^{-/-}$ mice than those seen in wt animals.

The results of these in vivo experiments indicate that AhR is responsible for the antiallergic and modulatory effects of M50367 on the Th1/Th2 balance.

Modulation effects of M50354 on in vitro Th1/Th2 differentiation from naive Th cells

The addition of M50354 suppressed IL-4 production by naive Th cells and modulated the naive Th cell differentiation into Th1/Th2 cells toward Th1 dominance (13).

Naive Th cells isolated from *AhR*$^{-/-}$ or wt mice were stimulated with anti-CD3 and anti-CD28 mAbs, and then incubated for 6 days in the presence or absence of M50354. We measured the levels of IL-4 and IFN-γ in culture medium by ELISA on day 3 to evaluate the effects of M50354 on early cytokine production, and conducted intracellular cytokine staining on 6 days after treatment to determine the proportions of differentiated Th1/Th2 cells. Addition of M50354 significantly suppressed IL-4 production (1.1–0.4 ng/ml) in wt mice (Fig. 4*A*). M50354 also significantly reduced the population of Th2 cells from 16.4 to 4.5% in these animals (Fig. 4*B*). In *AhR*$^{-/-}$ mice, however, neither IL-4 production nor the proportion of Th2 cells were altered by the addition of M50354 (Fig. 4). AhR-deficient mice exhibited 2- to 3-fold higher levels of both IL-4 and IFN-γ than those seen in wt mice (Fig. 4*A*), a phenotype that is likely associated with enhanced IgE production.

The results of these in vitro experiments indicated that the modulatory effects of M50354 on Th1/Th2 differentiation were mediated by AhR signaling and AhR is likely involved in regulation of the differentiation of naive Th cells into Th1/Th2 cells.

Involvement of AhR signaling in the modulation of Th1/Th2 differentiation

To investigate the role of AhR in the differentiation of naive Th cells, we investigated the expression of AhR throughout the course of Th cell differentiation. Naive Th cells prepared from C57BL/6 mice were stimulated with anti-CD3 and anti-CD28 mAbs. After